

# Design of anchoring at the top of slopes for geomembrane lining systems

L. Briancon, H. Girard And D. Poulain  
*Cemagref, Groupement de Bordeaux, Cestas Cedex, France*

N. Mazeau  
*Cemagref - CUST, University of Clermont-Ferrand, France*

*Keywords:* Geotextiles, Geomembranes, Anchorage, Testing, Design method

**ABSTRACT:** Geosynthetic lining systems are increasingly used for hydraulic works and waste landfills. These systems are not always stable in themselves on the slope and require anchoring at the top of the bank. The purpose of the research work undertaken by the Cemagref at the request of the CETMEF (Maritime and Fluvial Technical Research Centre) is to define a design method for anchoring at the top of slopes based on life-size tests. The results of the first tests performed with anchoring in sand are presented here. Different types of anchoring were tested, enabling a comparison with the theoretical calculation methods and providing knowledge on the effect of the different geometrical parameters of the trenches on the anchoring performance.

## 1 INTRODUCTION

Geosynthetic lining systems (GLS) are widely used in engineering structures such as dams, canals or waste landfills. They offer a worthwhile alternative to older solutions. Such systems include a geomembrane (GMB) which ensures the sealing of the structure. The GMB may be combined with geotextiles (GTX) and related products, the essential function of which is to provide its protection and/or drainage. A layer of soil is placed on the top GTX to enable, in certain cases, the re-planting of the slope with vegetation.

Because of essentially economic constraints, the current trend is towards to the vertical and lateral extension of the majority of the structures mentioned above. This results in adopting steep slopes, generating problems of slope stability, slippage, or failure of certain parts of the geosynthetic system (GSY).

In the majority of cases, the GSY complex generally presents a slip surface at the GMB/GTX interface, as the GMB has a low friction angle with the other materials. When the system is not stable in itself by simple friction, the upper GTX has to be anchored to prevent any slippage and to absorb the stresses induced by the top soil cover resting on the GSY complex, thus reducing the stresses on the GMB. Depending on the spatial constraints of the structure, anchoring can come in different forms, such as simple run-out or trenches of various geometrical patterns.

The review of the literature in this field has essentially highlighted two design methods which can give very different results depending on the configurations of the trenches studied.

The first method takes account only of the friction at the GSY/soil interface. The second, in addition to friction, integrates the angle effects in the anchoring trench.

We have designed an apparatus making it possible to model large anchoring trenches and to determine experimentally their anchoring capacity.

This paper presents the results of the series of tests performed with a single soil and two types of geotextiles, which made it possible to test three types of anchoring. This series of tests enabled us to verify the effect of the slope angle, to compare our results with the existing calculations, and to evidence certain important parameters for the designing of anchoring trenches at the top of the slope.

## 2 THE PROBLEM OF DESIGNING

### 2.1 Geometry of the trenches studied

There are numerous methods for anchoring GSY at the top of the slope. Three types been distinguished (Figure 1) :

- simple run-out on length L,
- partial anchoring or vertical embedding (L+D),
- complete anchoring (L+D+B).

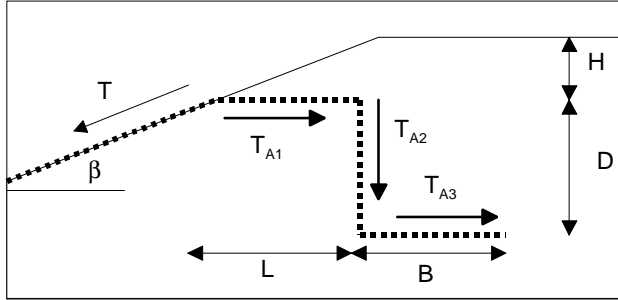


Figure 1. General shape of an anchoring trench

### 2.2 Taking account of friction alone

One design method, based on the hypothesis that the stresses at the level of the anchoring are absorbed solely by friction without any angle effect, has been presented by Koerner (1994). The calculation is made for a complete anchoring in trenches, but remains valid for other configurations.

Considering that the soils studied have no cohesion and that the layer of soil deposited on the length L moves with the GTX, we get :

$$T_{A1} = \gamma H L \tan \phi_{s,GTX} \quad (1)$$

$$T_{A2} = 2\gamma K_0 D \left( \frac{D}{2} + H \right) \tan \phi_{s,GTX} \quad (2)$$

$$T_{A3} = 2\gamma B(D+H) \tan \phi_{s,GTX} \quad (3)$$

$\gamma$  = specific weight of the soil

$\phi_{s,GTX}$  = friction angle at the soil/GTX interface

$K_0 = (1 - \sin \phi)$  at-rest earth pressure coefficient

The anchoring capacity of the trench studied is the sum of these three forces for a horizontal extraction of the GTX (Figure 1).

### 2.3 Influence of the slope angle

Koerner (1991-1994) proposed this method, taking account of the effect of the slope angle. He considers that the fact of pulling the GTX along the slope results in an increase in the normal constraint, increasing the friction force at the soil/GTX interface over the length L. By applying this method to simple run-out, he determines the increased anchoring capacity according to the following relation:

$$T = \gamma H L \tan \phi_{s,GTX} \left( \frac{1}{\cos \beta - \sin \beta \tan \phi_{s,GTX}} \right) \quad (4)$$

## 2.4 Taking account of the angle effects in the trench

Various designers have proposed that the friction on the flat parts of the trench and an additional resistant force at each corner of the trench should be taken into account. This additional force, based on the law of wires resting on a revolving cylinder, means that a multiplying factor, equal to  $e^{\lambda \cdot \tan \phi_{s,GTX}}$ , must be applied to the frictional force upon each change of direction, where  $\lambda$  is the angle of the change in direction and  $\tan \phi_{s,GTX}$  is the friction coefficient. (figure 2)

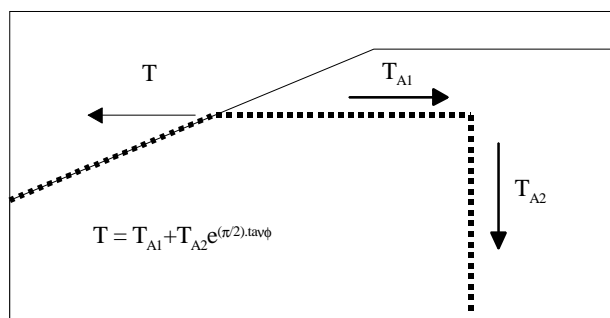


Figure 2. Effect of an angle on the anchoring capacity

With this approach, the corners of the trench absorb substantial stresses and increase the anchoring capacity calculated by simple friction.

## 2.5 Existing experiments

Very few experiments on anchoring trenches at the top of slope have been recorded. The tests performed *in situ* by Imaizumi (1997) on trenches filled with concrete to anchor geomembranes are worthy of note. These tests evidenced the various failure mechanisms dependent upon the nature of the geomembranes anchored and the dimensions of the trenches.

Mention can also be made of the tests of Koerner (1991) performed on geomembranes using a large scale laboratory pullout box which enabled him to determine a safety coefficient over the length of the GMB to be anchored.

These studies were performed on geomembranes, *in situ*, or by adapting existing laboratory apparatus. We considered that it would be interesting to design specific apparatus, consisting of an anchoring bench, enabling the modelling of geosynthetic anchoring trenches at the head of the slope in order to determine their anchoring capacity and to assess the various mechanisms governing such systems.

## 3 EXPERIMENTATION

### 3.1 Presentation of the anchoring test bench

The anchoring test bench (Figure 3) consists of an anchoring zone and of a traction device. The dimensions of the anchoring zone make it possible to model a soil mass and an anchoring trench with a maximum depth equal to 0.8 m and a run-out length of 1.2 m by one metre wide.

The traction device consists of a 50 kN winch and an angle drive bracket enabling the simulation of the traction forces following an angle determined in relation to the horizontal, within a range of values from  $0^\circ$  to  $35^\circ$ .

The traction device is connected to the GTX by a jaw coupled to a tensile cell indicating the force required to pull the GTX out of the trench.

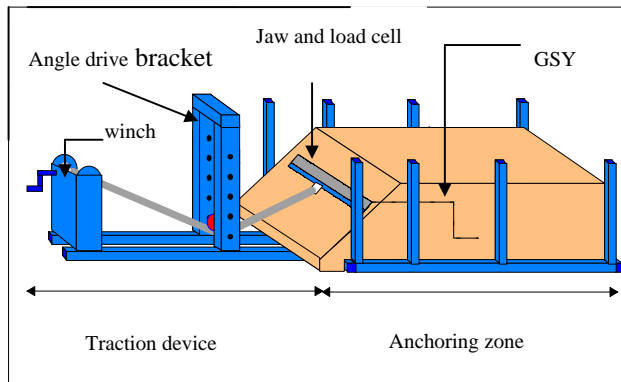


Figure 3. Diagram of the anchoring test bench

### 3.2 Materials used

The soil used for the first series of tests was 0/2.5 mm rolled sand. Its high internal friction angle ( $\phi_{s,s} = 40^\circ$ ) makes it possible to produce deep trenches and steep slopes.

During the development tests, a TP331 polypropylene GMB (called Mo1 in the rest of this paper) from the "Siplast" range was used, under a GTX. Two non-woven, needle-punched GTX materials from the "Bidim" range were tested :

- one protective GTX P50 (Xa2),
- one reinforcement GTX, Rock Peck 75 (Xa3).

Table 1 shows the friction angles at the interfaces of the various materials used.

Table 1. Different friction angles at the interfaces of the materials tested

	Sand	Xa3
Sand	40°	34°
Mo1	22°	16°
Xa2	34°	-
Xa3	34°	-

The GTX Xa2 was used for the run-out tests and for the tests on trenches with low anchoring capacity, thus requiring low traction on the GTX to pull it out of the trench. The high elongation at maximum stress of the GTX Xa2 and its medium tensile strength meant that it could not be used for the tests requiring high traction on the GTX (see Table 2). In such tests, the GTX Xa2 suffers from elongation over its length,  $L$ , and its contact area with the soil decreases in the course of the test, involving new parameters that are difficult to take into account. The GTX Xa3, which is stronger and less easily lengthened (see Table 2) was chosen to test the anchoring capacities of large trenches.

Table 2. Mechanical characteristics of the GTX tested

Type of GTX	Tensile stress (kN/m)	Tensile strain at failure (%)
Xa2	30	85
Xa3	75	11

### 3.3 Development tests

The various development tests resulted in modifying the experimental apparatus to enable better modelling of the anchoring trenches.

#### 3.3.1 Reduction of lateral friction

Implementation of the layer of soil over the length  $L$ , using shuttering removed prior to the application of traction on the GTX, made it possible to eliminate the lateral friction that is difficult to estimate.

### 3.3.2 Evidencing of failure along the slope

The first configuration of the bench included an abutment enabling a reduction in the volume of soil to be placed and an easier modification of the slope. Comparative tests with and without an abutment revealed that this plays an important part in increasing the anchoring capacity. This abutment was therefore eliminated, which furthermore made it possible to observe failures in the soil at the level of the slope for certain geometrical configurations.

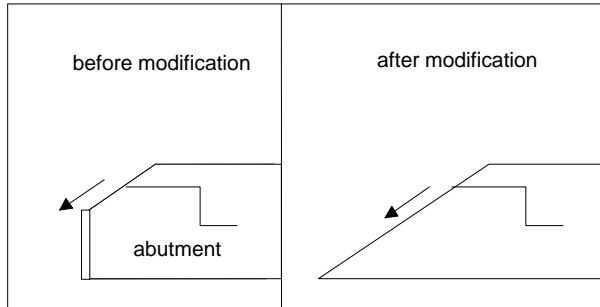


Figure 4. Modification of test apparatus

### 3.3.3 Increase of friction at the GST interfaces

The development tests were performed with the GTX Xa3 and with the GMB Mo1 being laid under the GTX. With the small friction angle at the GTX/GMB interface, it was impossible to obtain sufficiently high and sufficiently differentiated tensile forces to analyse the results. The tests were therefore carried out on a GTX (Xa2 or Xa3) without GMB. A higher friction angle increased the differences between the forces measured for the various cases tested.

### 3.4 Procedure

As a result of what was learned from the development tests, the following procedure was adopted :

- installation of the soil (reworking, compacting, levelling and layout of the slope),
- making of the trench,
- installation of the GTX in the trench,
- filling of the trench and overlapping (with compacting layer by layer),
- installation of the anchoring jaw and force sensor,
- application of traction to the GTX (Figure 5).



Figure 5. Photo of the implementation of an anchoring test

### 3.5 Series of tests

Three series of tests were performed, corresponding to three types of anchoring :

- tests with run-out alone over a given length L (1.5m) with horizontal traction of the GTX and traction along the slope by varying the angle of the slope from 0° to 30°,
- vertical embedding tests for two lengths L (0.5 and 1.1m) and three anchoring depths D (0,3 ; 0.6 and 0.9m),
- complete anchoring tests for one anchoring length L (1.1m), two depths D (0.3 and 0.6m) and two lengths of the bottom of the trench B (0.3 and 0.6m).

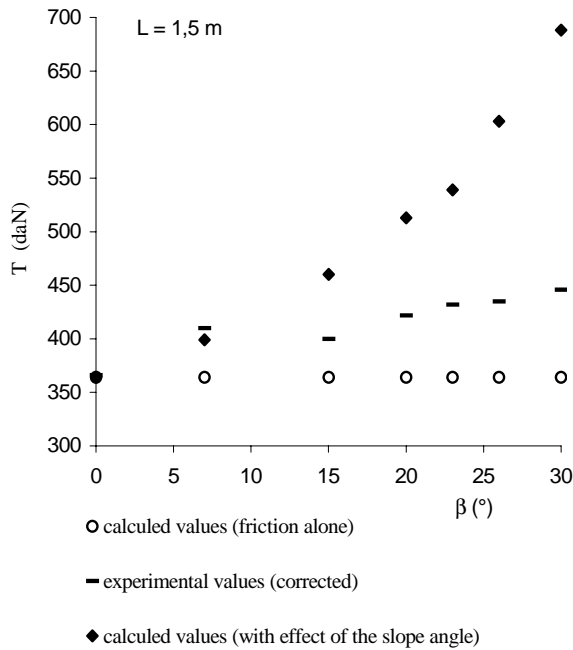


Figure 6. Graph comparing the experimental and calculated values for simple run-out

## 4 ANALYSIS OF THE VARIOUS RESULTS

### 4.1 Simple run-out tests (L)

The simple overlap tests were performed on seven slope angles with the GTX Xa2 . Some of these tests were performed three times to verify the repeatability of our experiments.

For greater accuracy with respect to the normal stress applied on the GTX, the soil resting on the GTX was weighed after each test and was applied in such a manner that there was no lateral friction with the walls of the anchoring bench during its movement in the course of the test (shuttering removed before testing).

Figure 6 shows the results of these tests and compares them to the values as calculated, taking into consideration : the friction alone and the effect of the slope angle. The experimental values presented in this figure are corrected values. They have in fact been brought back to an average soil weight, given that the conditions of implementation did not make it possible to have the same weight of soil at each test for the GTX. Table 3 shows the details of the soil weight for a few tests.

When comparing the experimental and calculated values from friction alone, it can be observed that the slope angle has an influence on the anchoring capacity of the simple run-out anchorage at the top of the slope, an influence which increases with the angle of the slope. Moreover, Figure 6 shows that, in our experimental conditions, the method proposed by Koerner to take account of this influence overestimates the anchoring capacity in the case of run-out alone.

Table 3. Experimental and calculated values for different slope angles

$\beta$ (°)	Raw exp. values	Corrected exp. val- ues	Soil weight	Calculated values (fric- tion alone)	Calculated values (slope)
0	359	364	532	364	364
	326	373	472		
	355	362	529		
	361	364	535		
15	439	400	592	364	460
22	437	432	546	364	539
26	435	435	527	364	603

#### 4.2 Vertical embedding tests (L+D)

The vertical embedding tests were performed with the GTX Xa2 for three anchoring depths. All the tests were repeated twice. For the embedding tests to a depth of 0.9 m, the forces measured did not correspond to the GTX extraction forces, as a failure in the soil was observed. In this case, the experimental values are to be taken, at most, to be equal to the anchoring capacity.

Figure 7 shows the results of the vertical embedding tests for a run-out length, L, of 0.5 m, and compares them to the results of the calculations taking only friction into account and to those using in addition the effect of the corners in the trench.

The values given by the calculation method taking only friction into account are on average 20% below the experimental values. This difference increases noticeably with the embedding depth. The following two additional hypotheses can be put forward to explain that :

the traction of the GTX along the slope results in a friction force  $T'_{A1}$  on the GTX (along the length L) greater than the friction force exerted on the GTX in the case of application of horizontal traction (cf. 4.1)

an increase in friction on D caused either by an additional horizontal constraint induced by the force  $T-T'_{A1}$  (figure 8.a), or by pressure applied to the soil at the corner of the trench (figure 8.b), this soil pressure being represented by a coefficient K .

Instrumentation of the trench would make it possible to determine what are the mechanisms governing such anchorings.

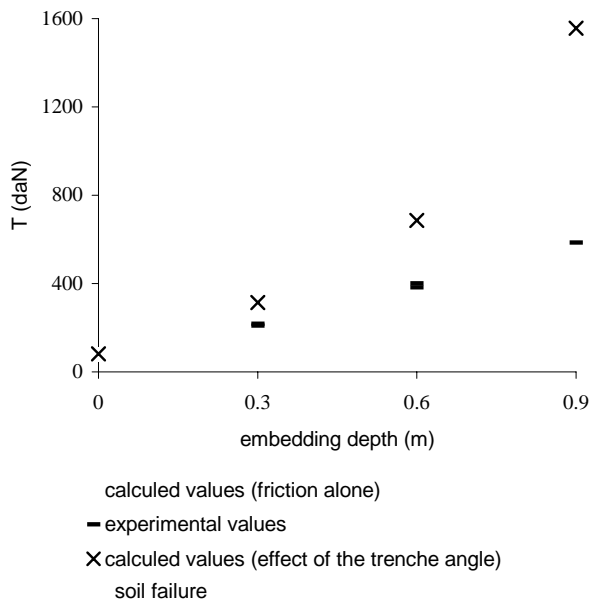


Figure 7. Graph comparing the experimental and calculated values for the case of vertical embedding

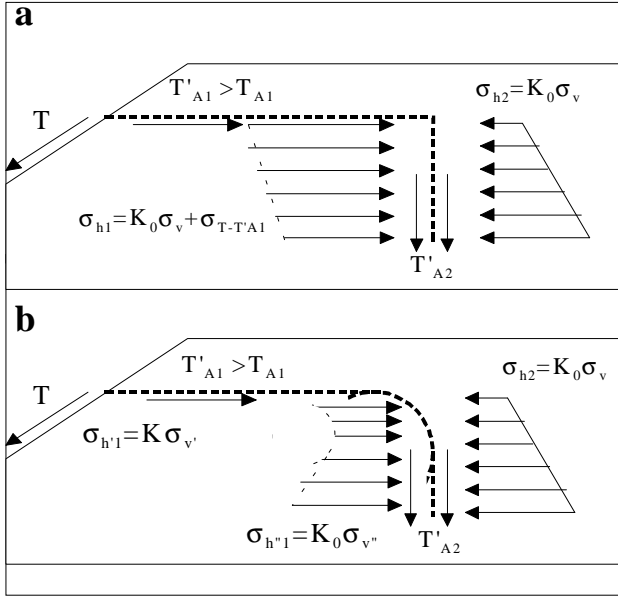


Figure 8. Various mechanisms explaining the differences observed between the experimental and calculated values

It appears clearly from figure 7 (and from table 5) that taking account of the effect of the corners of the trench by laws based on the theory of wires resting on a revolving cylinder considerably overestimates the anchoring capacity. In the case of anchoring with a complete trench, this method would apply to an additional corner and therefore overestimate all the more the anchoring capacity of the trench. For that reason, this design method will be abandoned for the third series.

#### 4.3 Anchoring tests in complete trenches ( $L+D+B$ )

To verify the influence of the various geometrical parameters of the trench on its anchoring capacity, a final series of tests was performed with the two GTX, Xa2 and Xa3, on complete trenches, by varying  $L$ ,  $D$  and  $B$ .

##### 4.3.1 Influence of $L$

For a given trench configuration ( $D$  and  $B$  fixed), the results of these various tests evidenced the existence of a minimum length,  $L$ , required to ensure the stability of the soil situated between the trench and the slope. Following the failure of the soil mass in one test ( $L=0.5m$ ;  $D=0.6m$  and  $B=0.3m$ ), we attempted to determine the failure line in the soil mass. The same test was therefore repeated, after columns of coloured sand had been arranged inside the mass. Following the failure, by cutting the soil mass along the plane of the coloured columns, we were able to observe the breaking of the columns and their displacement (Figure 9) and thus determine, for this configuration, the failure line. (Figure 10). This type of failure was also observed following the experiments of S. Imaizumi (1997) for certain small trenches ( $300 \times 300 \text{mm}^2$  and  $400 \times 400 \text{mm}^2$ ).

We are now going to estimate, by a simple calculation, the shear resistance,  $F_{\text{calculated}}$  of the soil mass along the failure line observed. The force  $F_{\text{calculated}}$  is calculated by projecting the forces applied to the soil mass situated between the trench and the slope (above the failure line) (eq.5) on the failure line determined by experimentation and on its normal direction (eq.6). By solving the two equations with relation 7, it is possible to calculate  $F_{\text{calculated}}$  according to the weight of the soil and the geometrical data of the problem.

$$P \sin \alpha + F_{\text{calculated}} \sin \beta \sin \alpha + F_{\text{calculated}} \cos \beta \cos \alpha = F \quad (5)$$

$$P \cos \alpha + F_{\text{calculated}} \sin \beta \cos \alpha + F_{\text{calculated}} \cos \beta \sin \alpha = N \quad (6)$$

$$F = N \tan \phi_{s,s} \quad (7)$$



where  $\alpha$  : angle of the failure line to the horizontal,  
 $\beta$  : angle of the angle of the slope,  
 $F$  : shear strength on the failure line,  
 $N$  : normal strength on the failure line,  
 $\phi_{s,s}$  : internal friction angle of the soil,  
 $P$  : weight of soils above the break line.

The force  $F_{\text{calculated}}$  is corrected by taking account of the lateral friction between the soil mass above the failure line and the walls of the anchoring bench.

The results obtained (Table 4) evidence that the measured force  $T_{\text{measured}}$  is close to the calculated force necessary to shear the soil mass,  $F_{\text{calculated}}$  and below the calculated force necessary to extract the GTX,  $T_{\text{GTX calculated}}$  (Table 4).

Table 4. Comparison of measured and calculated forces for the case of a failure in the soil mass

	$T_{\text{measured}}$	$F_{\text{calculated}}$	$T_{\text{GTX calculated}}$ (friction only)
Test A	700 daN	Failure line is	not determined
Test B	774 daN	740 daN	817 daN

Following these two tests, the anchoring capacity would therefore appear to be limited by a shear strength of the soil mass and that a minimum length,  $L$ , must be determined for a given force to be anchored. These two tests, with a break in the soil mass, made it possible to evidence this phenomenon. They must be followed by further tests to propose a method to determine  $L$  according in particular to the type of soil, to the GSY used and to the geometrical configuration of the trench.

#### 4.3.2 Influence of $D$ and of $B$

Figure 11 and table 5 present the influence of the depth of anchoring,  $D$ , and of the size of the bottom of the trench,  $B$ , for a length  $L$  (distance between the trench and the slope) equal to 1.1 m assuring the stability of the soil mass.

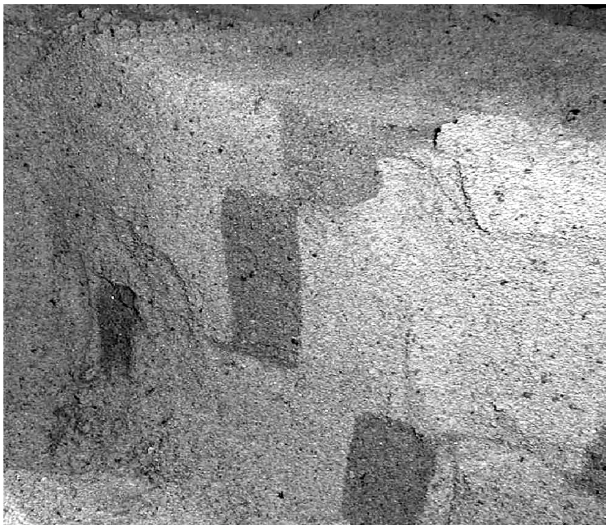


Figure 9. Photo showing the breaking and the displacement of the columns of coloured sand

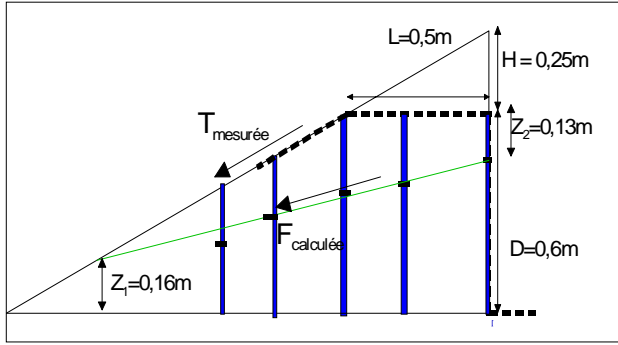


Figure 10. Failure observed by experimentation

Any variation of  $D$  has an effect on the friction force applied to the vertical wall of the trench, but also to that applied in the bottom of the trench (cf. equations (2) and (3)).

For a shallow depth ( $D = 0.3\text{m}$ ), the anchoring capacity measured experimentally is slightly lower than that calculated by the method taking only friction into account. This may be explained by the fact that the corners of the trench become rounded in the course of the tensioning of the GTX, which alters the geometry of the trench.

For a greater depth ( $D=0.6\text{m}$ ), the rounding of the corners does not alter the overall geometry of the trench, which keeps a vertical part. In this case, the values calculated from equations (1), (2) and (3) taking solely friction into account are smaller than the measured values

Generally speaking, on the basis of the calculation with friction alone, the anchoring capacity of the trench alone ( $D+B$ ) represents over 80% of the total capacity of the system at the top of the slope ( $L+D+B$ ).

The geometrical parameters to be taken into account in design such trenches are the depth of the trench,  $D$ , and the size of the bottom of the trench,  $B$ . The length  $L$  must essentially be taken into account to ensure the stability of the soil mass between the trench and the slope.

By comparing in figure 11 the measured and calculated values (friction alone) of  $T$  for different tests in complete trenches made with different size for the bottom of the trench,  $B$ , (0.3 and 0.6m) and with identical depths,  $D$ , it appears that the force  $T_{A3}$  can be attributed to friction alone (for example,  $\Delta T_1 \approx \Delta T_2 \approx \sigma_V \tan \phi_{s,GTX}$  in figure 11).

Table 5. Summary of the various results of the trench anchoring tests

	L (m)	D (m)	B (m)	GTX	Exp. values (daN)	Calculated values 1 (daN)	Calculated values 2 (daN)
Partial trench	0.5	0.3	0	Xa2	210	150	314
		0.6			218	301	686
		0.9			401	518	1557
	1.1	0.3	0	Xa2	383	518	1557
		0.6			593*	518	1557
		0.6		Xa3	586*	771	
Complete trench	0.5	0.6	0.3	Xa2	370	302	466
	1.1	0.3			757	453	902
			0.6	792	453	902	
		0.6	Xa3	771			
			0.6	Xa2	771		
	Complete trench	0.5	0.6	0.3	Xa2	750*	817
774*							
1.1		0.3	0.3	Xa2	595	636	
					835	970	
		0.6	0.3	Xa2	1159	969	
					1136		
0.6	Xa3	1780	1504				

failure in mass soil

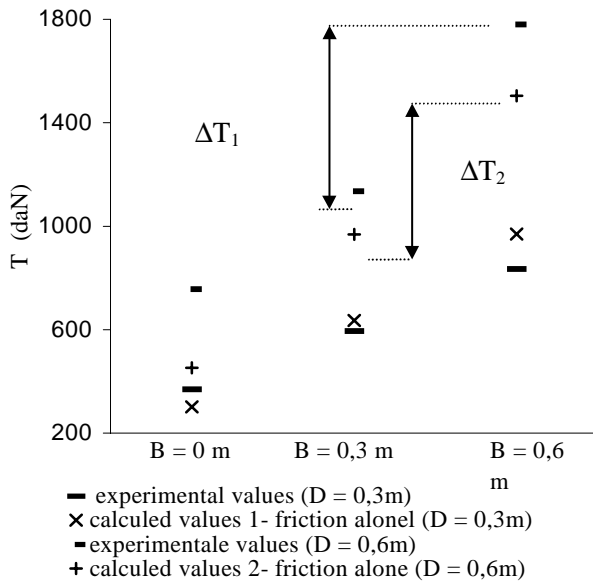


Figure 11. Influence of D depending on the anchoring configuration

## 5 CONCLUSION

In the experimental conditions implemented, in particular for the sand used, the series of tests performed on the anchoring bench evidenced that the calculation method taking account of an effect of the corners of the trench considerably overestimates the anchoring capacity of a given trench. Under the same conditions, the method taking account solely of friction underestimates the sizing of the anchoring capacity.

Following the tests with run-out anchor alone, we observed a slightly increase in the friction force applied to the GTX due to traction along the slope.

The test with vertical embedding resulted in various hypotheses on the mechanisms governing such trenches which may be the origin of the difference between the experimental values observed and the calculated values (calculation method taking only friction into account). These tests also evidenced the existence of a minimum anchoring depth, about to 0.3 m for our materials, as from which the trench anchoring solution becomes better than that using run-out alone.

The anchoring tests with a complete trench evidenced that :

- the stability of the soil mass at the top of the slope is ensured as from a minimum length, L,
- the forces applied to the GTX at the bottom of the trench correspond only to the forces of friction,
- there is a minimum length, B, equal to 0.3 m for our materials, as from which complete trench anchoring has a greater efficacy than that of vertical embedding.

As a result of the observations made in our experimentation, an approach for a method of designing anchoring trenches at the top of the slope may consist of :

- calculating the force to be absorbed at the top of the slope,
- determining the parameters D and B enabling this force to be absorbed by the anchoring,
- determining the length L between the trench and the slope ensuring the stability of the soil mass at the top of the slope.

This series of tests needs to be complemented in the following directions :

- tests with different soils (fine and coarse soils),
- instrumentation of the trench to improve understanding of the phenomena,
- evaluation of the safety coefficients.

## ACKNOWLEDGEMENTS

We should like to thank the producers (Bidim - Mr. O. ARTIERES and Siplast - Mr. G. POTIE) who provided the geotextiles and geomembranes and brought their own experience in this field of anchorage.

## REFERENCES

- Girard H., Poulain D. 1997. Stabilité des protections des dispositifs d'étanchéité par géomembrane dans les canaux de navigation. *Rapport interne Cemagref Bordeaux - STCPMVN*.
- Hullings D.E., et Sansone L.J. Design concerns and performance of geomembrane anchor trenches. *Geotextiles and Geomembranes*, 1997, vol 15, p. 403-417.
- Imaizumi S., Tsuboi M., Doi Y., Shimizu T. et Miyaji H. Anchorage ability of a geosynthetic liner buried in a trench filled with concrete, In : Sardinia 97, Sixth International Landfill Symposium, Cagliari, Italy, 13-17 October 1997. Cagliari : Environmental Sanitary Engineering Centre, 1997. p. 453-462.
- Koerner R.M. and Wayne M.H. *Geomembrane, Identification and performance testing*. Rilem report 4, Chapman and Hall (1991), pp 204-218.
- Koerner R.M. *Designing with geosynthetics*. Prentice-Hall, Inc., Englewood Cliffs, N.J, 1994. 783 p.
- Lalévée E., Briançon L., Girard H., Poulain D. 1999. Dispositifs d'étanchéité par géomembrane : dimensionnement des ancrages en tête de talus. *Rapport interne Cemagref Bordeaux - STCPMVN*.